Comparative study of the electronic structure of ordered, partially ordered, and disordered phases of the Cu_3Au alloy

J. Kudrnovský
Max-Planck-Institut für Festkörperforschung, Heisenbergstrasse 1, D-7000 Stuttgart 80, Federal Republic of Germany and Institute of Physics, Czechoslovak Academy of Sciences, Na Slovance 2, CZ-1801 40 Prague 8, Czechoslovakia

S. K. Bose
Max-Planck Institut für Festkörperforschung, Heisenbergstrasse 1, D-7000 Stuttgart 80, Federal Republic of Germany and Department of Physics, Brock University, St. Catharines, Ontario, Canada L2S 3A1

O. K. Andersen
Max-Planck-Institut für Festkörperforschung, Heisenbergstrasse 1, D-7000 Stuttgart 80, Federal Republic of Germany
(Received 30 July 1990)

We present a theoretical study of the electronic structure of ordered, partially ordered, and disordered phases of the Cu_3Au alloy using the scalar-relativistic linear muffin-tin orbitals (LMTO) method in conjunction with the coherent-potential approximation. We study the change in the electronic structure caused by the gradual increase of disorder in the alloy by varying the long-range-order parameter S continuously from its maximum ($S=1$) to the minimum ($S=0$) possible value. Calculations for the disordered phase ($S=0$) are performed with and without relaxation of the lattice. The relaxed-lattice calculation takes into account, in an approximate way, the possible deviations from the ideal lattice structure due to the difference in the sizes of the constituent atoms. As a side issue, we address the problem of transferability of the LMTO parameters of the individual alloy components in the pure crystalline phase to the alloy calculation.

I. INTRODUCTION

The electronic properties of ordered and disordered phases of the Cu_3Au alloy have been studied both experimentally[1-6] and theoretically[1,7-12] during the past few years. There are several reasons for the interest in this alloy: (i) The Cu-based alloys provide an important test example for the theories of allow phase stability based on the knowledge of the underlying electronic structure. (ii) The Cu_3Au system is the canonical example of an alloy which undergoes the order-disorder phase transformation. (iii) There are important relativistic effects related to the Au atoms. (iv) The d-valence states of Cu-rich alloys with the noble and the late transition metals are fully occupied, justifying a one-electron description (as opposed to, e.g., the case of partially filled d band of Ni where many-body effects are important). The occupied valence states are amenable to experimental studies via the techniques of photoemission and x-ray spectroscopy.[1-6]

The Cu-rich Cu-Au alloys, like the Cu-rich Cu-Pd alloys, are interesting from another point of view. In both alloys there are non-negligible lattice relaxation effects connected with the introduction of large impurity atoms (Pd or Au) into the matrix of the smaller Cu atoms. The fractional change in the equilibrium lattice constant $(a^Q-a^{Cu})/a^Q$, is 7% and 11% for Q=Pd and Au, respectively. To discuss qualitatively the possible influence of the size difference of the atoms on the electronic structure of Cu-rich alloys let us consider first a single Pd or Au impurity atom in the Cu matrix. Let us consider the single-muffin-tin (MT) approximation,[13] which uses a common MT radius for the host and the impurity atoms (i.e., Pd or Au MT radius equal to the Cu MT radius in this case). In the single site charge self-consistent calculation there is a tendency to screen the impurity potential as much as possible since only the potential in the impurity MT sphere is perturbed. The perturbation in all the remaining MT spheres as well as the interstitial space is neglected. The impurity becomes overscreened due to the limited space where self-consistency is performed. As a result, the impurity potential becomes more attractive and the d states are shifted to lower energies.[13] The situation is similar in random alloys studied by the self-consistent Korringa-Kohn-Rostoker–coherent-potential approximation (KKR-CPA) method: we have an impurity atom embedded in an effective (CPA) medium which is Cu-like for the Cu-rich alloys. The effect is less pronounced in comparison with the single impurity case as the common MT radii are slightly greater than the pure crystal Cu-radius in case of Cu-rich alloys. The second effect is the lattice expansion around the impurity, which has been confirmed by extended x-ray-absorption fine structure (EXAFS) measurements[13,14] for Cu-rich alloys. The actual impurity-host distance is underestimated in the single MT model. Consequently, both the

impurity-host hoppings and the impurity bandwidths are overestimated.[13] This effect is stronger in random Cu-rich alloys because of the nonzero probability of finding two Pd (Au) atoms as the nearest neighbors. In the single-impurity limit, these constraints of the single-MT model can be removed by allowing charge transfer outside the impurity MT sphere. One performs self-consistent calculations on a cluster consisting of the impurity MT sphere and the surrounding nearest Cu MT spheres which are shifted outwards to accommodate the larger impuity atom.[13] Such a program cannot be, at least at the present time, extended to concentrated alloys within the KKR-CPA formalism.

We have demonstrated recently that in the CPA (Refs. 15–17) version of the tight-binding–linear muffin-tin orbitals (TB-LMTO) method[18,19] approximate treatments of both charge self-consistency and lattice-expansion effects are possible. The method offers the option to choose different radii for the host and the impurity atoms. We use the atomic-sphere approximation (ASA) version of the LMTO method, in which the space is divided into volume filling, and hence (slightly) overlapping Wigner-Seitz (WS) spheres centered at the lattice sites and inside these spheres the charge density and the potential are approximated by their spherical averages. The ASA is a reasonable approximation, provided that there are very few electrons in the interstitial region. As a rule of thumb errors due to the ASA are small as long as the WS spheres, filling the electron containing parts of space, do not overlap more than 30%, i.e., $s^R+s^{R'}-|\mathbf{R}'-\mathbf{R}|<0.3s^R$ for all $\mathbf{R}$, where s^R is the radius of the sphere at site $\mathbf{R}$.[19] Sphere radii for the alloy constituents (Cu and Au atoms in the present case) can be chosen to be different so that the spheres are approximately neutral. A first guess for the sphere radii alloys obeying Vegard's law reasonably well (e.g., Cu-Au and Cu-Pd alloys) is the radii for the pure metals.[17,19] For Cu-Au and Cu-Pd alloys this choice of sphere radii leads to approximately neutral spheres, while the sphere overlaps stay within 30%. One can vary the sphere radii slightly about the pure component values to obtain perfectly charge neutral spheres. The TB-LMTO-CPA procedure (with neutral spheres) that we follow has the following advantages: (i) For an ordered alloy we automatically rule out the need to calculate the Madelung potential. (ii) The species potentials of neutral spheres, which are related to a common zero of energy within the ASA, are properly positioned with respect to each other on the energy axis. This is of central importance for the alloy calculation and it permits us to avoid, in the first approximation, a fully charge self-consistent calculation. (iii) The potentials in the spheres with radii slightly different from that of the pure components can be calculated trivially by considering the tabulated values of the potential parameters and their volume derivatives.[20] Thus no self-consistent calculation for the new radii are necessary. Thus the procedure offers the computational ease of an empirical TB scheme and the accuracy of a first-principles method. (iv) The variations in the interatomic distances can be modeled accurately via the variations in the TB-LMTO hopping integrals which are related unambiguously to the WS radii. The TB-LMTO-CPA method treats the off-diagonal disorder on the same footing as the diagonal or level disorder.[16,17]

Using the approach outlined above we calculate the electronic structure of both ordered and disordered phases of the Cu_3Au alloy. In the disordered phase we consider two limiting models of lattice expansions: (i) The nearest-neighbor distances Cu-Cu, Cu-Au (Au-Cu), and Au-Au are all chosen to be the same (unimodal distribution). This is the model commonly used in the KKR-CPA method. (ii) The nearest-neighbor distances are different (trimodal distribution) and approximately equal to the arithmetic averages of the corresponding pure consituent ones. The possible lattice relaxations are included only in the latter model. A comparison of the results obtained in the two models illustrates the effects of lattice relaxations on the electronic structure.

The Cu_3Au alloy is the canonical example of an alloy showing the order-disorder transition. In the ordered phase the underlying face-centered cubic (fcc) lattice with halved lattice constant is decomposed into four interpenetrating simple cubic (sc) lattices, of which three are occupied by Cu atoms and the remaining one by Au atoms. Each Au atom has twelve Cu nearest neighbors. In the completely disordered phase all four sc sublattices are occupied with probability 0.75 (0.25) by Cu (Au) atoms. Partially ordered structures with varying degrees of (dis)order exist between the two limiting cases, depending on the temperature and the thermal history of the sample. The degree of order can be described by a continuous variable S, the long-range-order (LRO) parameter.[21] The LRO parameter is linearly related to the probability of finding atoms at the correct positions and varies between the limits $S=0$ for the completely disordered to $S=1$ for the completely ordered alloy. It can be determined experimentally from the intensity of the superlattice lines. Since the origin of the interatomic interactions that are responsible for the ordering tendecy is electronic, a reliable study of the variation of the electronic structure with atomic arrangements is of central importance for the explanation of the phase diagram of these alloys. The determination of the dependence of the electronic structure of the $Cu_{75}Au_{25}$ alloy on the LRO parameter S is another aim of the present work.

In the ordered Cu_3Au phase we perform self-consistent LMTO calculations and compare the results with those obtained by using the parameters transferred from the pure components. This allows us to discuss the transferability of the LMTO parameters from the pure crystal phase to the alloy calculation. A similar study of the transferability of the parameters for use in the calculation for the completely disordered alloy (with lattice relaxations included) is also presented.

II. THEORY

Our alloy Hamiltonian in the orthogonal LMTO representation[18–20] has the form

$$H_{\mathbf{R}L,\mathbf{R}'L'}=C_{\mathbf{R}L}\delta_{\mathbf{R}\mathbf{R}'}\delta_{LL'} + \Delta^{1/2}_{\mathbf{R}L}[(S^0(1-\gamma S^0)^{-1}]_{\mathbf{R}L,\mathbf{R}'L'}\Delta^{1/2}_{\mathbf{R}'L'}\,, \quad (1)$$

where $\mathbf{R}$ is the site index of the underlying fcc lattice. The orbital quantum number L [$\equiv(l,m)$] has $l \leq 2$, i.e., we use the sp^3d^5 LMTO's on each site. The fcc lattice is formed of four interpenetrating sc sublattices. For $0<S\leq 1$ these sublattices are distinct and our problem has a 36×36 format. The probabilities p_ν^Q of finding the atom Q=Cu or Au on the sublattices ν=Cu, Cu, Cu, or Au are[21]

$$p_{\mathrm{Cu}}^{\mathrm{Cu}}=(3+S)/4,\quad p_{\mathrm{Cu}}^{\mathrm{Au}}=(1-S)/4\ ,$$
$$p_{\mathrm{Au}}^{\mathrm{Cu}}=3(1-S)/4,\quad p_{\mathrm{Au}}^{\mathrm{Au}}=(1+3S)/4\ . \tag{2}$$

In the ordered phase $S=1$, and $p_{\mathrm{Cu}}^{\mathrm{Cu}}=p_{\mathrm{Au}}^{\mathrm{Au}}=1$, $p_{\mathrm{Au}}^{\mathrm{Cu}}=p_{\mathrm{Cu}}^{\mathrm{Au}}=0$. On the contrary, in the completely disordered phase $S=0$, and $p_{\mathrm{Cu}}^{\mathrm{Cu}}=p_{\mathrm{Au}}^{\mathrm{Cu}}=0.75$, $p_{\mathrm{Cu}}^{\mathrm{Au}}=p_{\mathrm{Au}}^{\mathrm{Au}}=0.25$, and all sublattices are equivalent. Thus for the $S=0$ case the problem has only a 9×9 format.

The structure of the underlying fcc lattice enters the Hamiltonian (1) via the structure constant matrix S^0, which is independent of the lattice constant (it depends[19] on the dimensionless quantity $d=|\mathbf{R}-\mathbf{R}'|/W$, where W is the alloy WS radius). The properties of the atoms which occupy th elattice sites are characterized by the potential parameters[19] $X=C$, Δ, and γ, which are matrices with elements X_{RL}, diagonal with respect to the indices $\mathbf{R}$ and L. In the alloy the potential parameters take on randomly two different values of X_L^Q (Q=Cu,Au), with probabilities p_ν^Q given by Eq. (2) on each of the four sublattices. The parameters X_L are obtained from the solutions to radial Schrödinger equation for the Cu and Au local-density approximation (LDA) potentials evaluated in the WS spheres with radii s^{Cu} and s^{Au}, respectively. The hopping integrals $H_{\mathbf{R}L,\mathbf{R}'L'}$ are thus directly and unambiguously related to the WS radii of the constituent atoms or, equivalently, to the interatomic distances.

In the ordered phase ($S=1$) we use either the potential parameters obtained from the self-consistent calculations performed at the experimental alloy volume or the tabulated potential parameters[20] for the pure Cu and Au metals appropriately modified for their slightly different radii in the alloy (as required by volume preservation in the alloy) using the tabulated values of the volume derivatives[20] (for details we refer to Ref. 19; see also Refs. 15 and 17). To correct for the fact that the Cu_3Au alloy WS radius W differs from the radii s^Q (Q=Cu or Au) we must multiply the parameters Δ_l^Q and γ_l^Q by the factor $\lambda_l^Q=(s^Q/W)^{2l+1}$. The use of these same potential parameters in the disordered phase ($S=0$) amounts to completely neglecting the lattice relaxation effects.[15,17] To incorporate the lattice relaxation we approximate the structure constant for the deformed (relaxed) lattice between the sites $\mathbf{R}$ and $\mathbf{R}'$ occupied by atoms Q and Q' by $\mu_l^Q S^0_{\mathbf{R}L,\mathbf{R}'L'}\mu_{L'}^{Q'}$, where $\mu_l^Q=(W/s^Q)^{1+l/2}$ and S^0 is the undeformed (ideal lattice) structure constant. This expression is derived on the assumption that the distances $d^{\mathrm{Cu\text{-}Cu}}$ and $d^{\mathrm{Au\text{-}Au}}$ are close to those in the pure crystals and the distances $d^{\mathrm{Cu\text{-}Au}}=d^{\mathrm{Au\text{-}Cu}}$ are approximately equal to the arithmetic average of the distances $d^{\mathrm{Cu\text{-}Cu}}$ and $d^{\mathrm{Au\text{-}Au}}$. For values of the radii s typical for transition metals the arithmetic average is close to the geometric average, from which the above result follows. We also assume that the distances $d^{QQ'}$ between sites $\mathbf{R}$ and $\mathbf{R}'$ depend only on these sites and their occupants, and that they are not influenced by other sites (for further details see Refs. 15 and 17). This is certainly an approximation, but it can give us a feeling as to the importance of the lattice relaxation effects in the alloy under study.

The next point concerns the choice of the sphere radii necessary to make the Cu and the Au spheres charge neutral. We proceed in the following manner. As stated above the choice of the pure crystal radii is already a good staring point for alloys obeying Vegard's law, of which Cu_3Au is an example. Starting with this choice we perform CPA calculations with the Hamiltonian (1) and determine local densities of states (LDOS) on Cu and Au atoms as well as the total alloy DOS. Once the alloy Fermi level E_F is found from the total DOS, we calculate the local charges q^Q (Q=Cu,Au) by integrating the Cu and Au LDOS up to E_F. The corresponding deviations from the sphere neutrality are $\delta_q Q=11-q^Q$. Charge conservation requires $\delta q^{\mathrm{Au}}=-3\,\delta q^{\mathrm{Cu}}$. To make, for example, the Au sphere charge neutral, we can set $\delta q^{\mathrm{Au}}=-4\pi(s^{\mathrm{Au}})^2 n^{\mathrm{Au}}\delta s^{\mathrm{Au}}$, where n^{Au} is the tabulated[20] electron density evaluated at the WS radius s^{Au}. The related quantity δs^{Cu} is obtained from alloy volume conservation $3(s^{\mathrm{Cu}}+\delta s^{\mathrm{Cu}})^3+(s^{\mathrm{Au}}+\delta s^{\mathrm{Au}})^3=W^3$, where W is the alloy WS radius. We then calculate the new potential parameters for the new radii $s^Q+\delta s^Q$ using the tabulated values of the volume derivatives,[20] and repeat all steps. Usually after one or two iterations the charge deviations δq^Q are negligible (less than 0.01 electrons per site).

We note that approaches similar in spirit, although different in technical details, were proposed recently.[22,23] In Ref. 22 the relative positions of the d resonances in amorphous Zr-Cu alloys were determined by self consistently adjusting the diagonal elements of an empirical TB Hamiltonian demanding zero charge transfer between Zr and Cu atoms. In Ref. 23 the TB parameters for Si were extracted by rescaling the energy functional in a physically transparent manner, and self-consistency was approximated within the TB model by enforcing atomic charge neutrality using a simple algorithm. In our method we vary the sizes of the atomic spheres until they contain the proper number of valence electrons in order to be charge neutral. Differences in the sizes of the atomic spheres induce lattice relaxation, which is incorporated in the calculation by appropriate modifications of the hopping integrals as discussed earlier.

The final remark concerns the choice of the potential parameters X^Q ($X=C,\Delta,\gamma$ and Q=Cu,Au) for the partially ordered alloys ($0<S<1$). For the potential parameters we use linear interpolation between the limits $S=1$ and 0 discussed above, so that $X_L^Q=(1-S)X_L^Q(S=0)+SX_L^Q(S=1)$. These S-dependent potential parameters form the input of the CPA equations.

The derivation of the CPA equations and their solutions were discussed in Refs. 16 and 17 for the case of simple lattices (one atom per unit cell). The formalism can be generalized straightforwardly to the case of many atoms per unit cell (as in the case of the partially ordered

Cu_3Au alloy). We obtain a set of coupled CPA equations with the symmetries $L = s,p,t_{2g},e_g$ on Cu and Au sublattices of the Cu_3Au lattice with different sublattice concentrations of Cu and Au atoms given by Eq. (2). The method of solution of these equations remains the same as before,[17] but the computer time requirement increases significantly (the problem has a dimensionality four times larger than the case of one atom per unit cell).

III. RESUTS AND DISCUSSIONS

In this section we present the results for the ordered and disordered phases of the Cu_3Au alloy. The latter case is studied both with and without the lattice relaxation. Also, we present the results for the alloy with LRO and discuss the transferability of the LMTO parameters from the pure crystal to the alloy calculation for both the ordered and the disordered phases.

A. The ordered Cu_3Au alloy

We have determined self-consistent scalar relativistic LMTO-ASA potential parameters for the ordered Cu_3Au alloy using an *spdf* basis. In Sec. III D we compare these parameters with those appropriately transferred from the pure crystalline phase parameters, obtained with the same basis and tabulated in Ref. 20. Calculations were performed for both equal Cu and Au radii (consistent with the experimental lattice constant of the alloy), as well as for different Cu and Au radii according to the prescription of Ref. 19. (The latter yields values

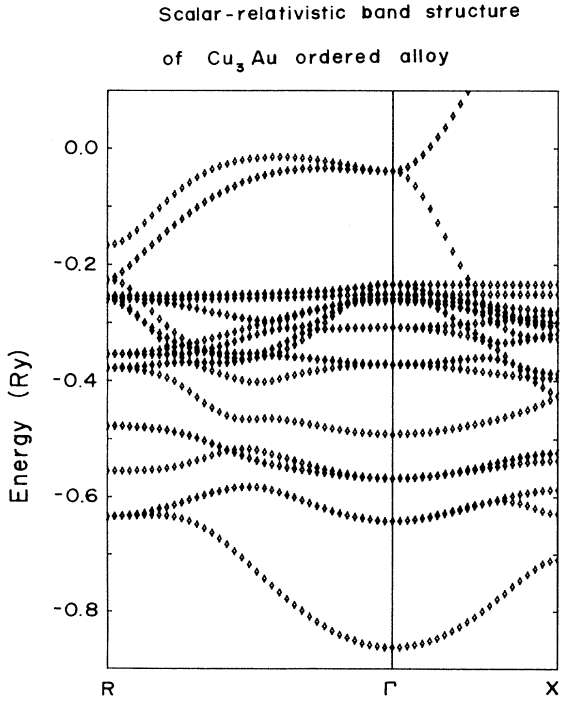

FIG. 1. Scalar-relativistic band structure of the ordered Cu_3Au alloy along the line $L-\Gamma-X$ in the Brillouin zone of the simple-cubic lattice.

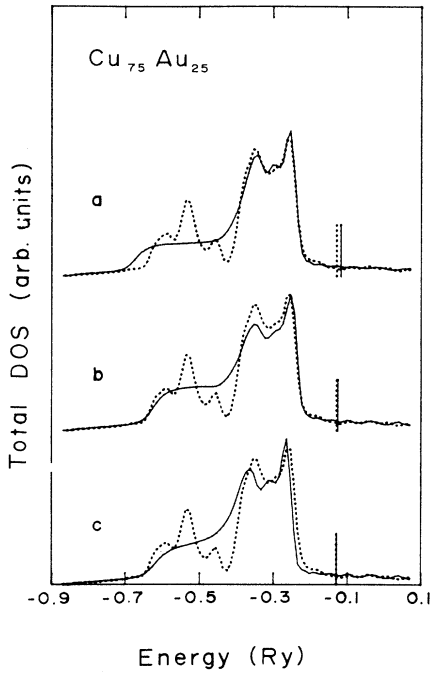

FIG. 2. Total density of states for the disordered $Cu_{75}Au_{25}$ alloy. Case (a): the effect of the lattice relaxations neglected. Case (b): the effect of the lattice relaxations included. Case (c): the same as case (b), but in addition the Cu and Au spheres were made neutral. The long vertical lines denote the positions of the alloy Fermi level. The results are compared with the ordered Cu_3Au alloy case (dotted lines).

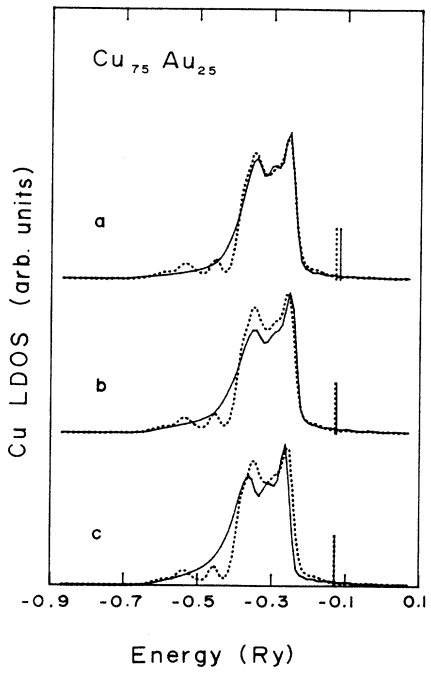

FIG. 3. Same as in Fig. 2, but for the local Cu density of states (not concentration weighted).

$s^{Cu}=2.670$ a.u. and $s^{Au}=3.012$ a.u., which are essentially the pure-crystal values, $s^{Cu}=2.667$ a.u. and $s^{Au}=3.002$ a.u.,[19] as Vegard's law is well fulfilled for the Cu_3Au alloy.) The energy bands are the same in both cases within the numerical accuracy, but the charge transfer among spheres of equal radii is significantly greater than in the other case. This indicates the importance of the proper choice of the component sphere radii in the disordered phase, especially if the calculations are not charge self-consistent. As we have discussed in the Introduction, the proper choice of sphere radii is important even in the self-consistent version of the CPA.

The band structure along the $R-\Gamma-X$ line in the sc Brillouin zone is plotted in Fig. 1. It agrees with that in Ref. 8 and, with the exception of the lifting of some degeneracies due to the spin-orbit effect, also with those in Refs. 7 and 11. The d-band width is not influenced by the spin-orbit effects. We note that the d bands at $E\in(-0.65,-0.45)$ Ry are predominantly due to the Au states, while those at $E\in(-0.4,-0.25)$ Ry are due to the Cu states. This is clearly seen from the plots of the total DOS, Fig. 2, and its decomposition into the Cu contribution (Fig. 3) and the Au contribution (Fig. 4). Our results agree well with those obtained previously by the LMTO (Refs. 1 and 9) as well as by the linear combination of Slater orbitals[8] methods. We only note the smaller energy resolution of our curves due both to the larger energy step (0.01 Ry) used in our calculation and to the method of Brillouin zone integration (the calculations were performed with the energy axis shifted into the complex plane followed by analytical deconvolution back to the real axis at the end[17]). The effect of the spin-orbit coupling[10,11] is to split $d^{3/2}$ and $d^{5/2}$ states, which leads to some shape changes, especially in the lower part of the spectra dominated by the Au states, while leaving the bandwidth essentially unchanged.

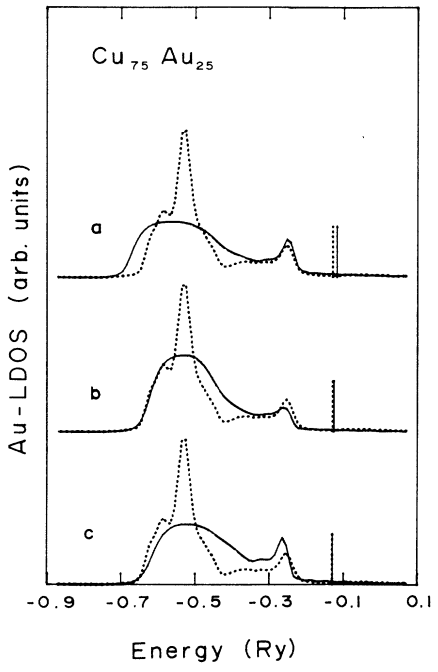

FIG. 4. Same as in Fig. 2, but for the local Au density of states (not concentration weighted).

B. The disordered $Cu_{75}Au_{25}$ alloy

The results for the total and component DOS plotted together with the ordered Cu_3Au counterparts for the sake of comparison are displayed in Figs. 2–4. We have performed calculations neglecting the lattice relaxations [case (a)] as well as including the lattice relaxation effects [case (b)], both based on the parameters derived from the self-consistent ordered Cu_3Au calculation. We find a small charge transfer, of the order of 0.1 electron per Cu site. We also present the results for the neutral spheres with radii $s^{Cu}=2.705$ a.u. and $s^{Au}=2.926$ a.u. [case (c)]. While the qualitative features of the DOS are the same in all cases, we clearly see the band narrowing due to lattice relaxations. This band narrowing is consistent with the pronounced differences observed in the local Au DOS with and without the lattice relaxations (while the local Cu DOS remains essentially unchanged). The reason for this narrowing in the model including lattice relaxation can be easily understood. The Au-Au nearest-neighbor distance in this model is close to its value in the pure crystal, and thus greater than in case (a), where it is assumed that all nearest-neighbor distances are equal and correspond to the average nearest-neighbor distance in the alloy. Consequently, the Au-Au as well as the Au-Cu nearest-neighbor hopping integrals are overestimated in case (a), resulting in broader local Au DOS. A similar effect was found in our recent calculation for Cu-rich Cu-Pd alloys,[15] and is supported by recent angle-integrated photoemission (PES) data,[14] which allows one to extract the component LDOS (through the use of difference photon-energy dependence and the Cooper minima of the atomic matrix elements of the consituent atoms in the alloy). Recent angle-integrated PES experiments in ordered and disordered Cu_3Au alloys[5] point to the superiority of models (b and c) over model (a). These experiments clearly show that the bandwidths for the ordered and the disordered phases are the same, just as found in our models (b) and (c). On the contrary, the KKR-CPA calculations,[1,9–11] based on models that neglect lattice relaxation, overestimate the bandwidth in the disordered phase, while giving excellent agreement for the ordered case.[5]

It is worth pointing out that the angle-integrated PES data are not, strictly speaking, proportional to the total DOS but rather to the concentration and matrix-element-weighted local DOS. The matrix elements of Cu and Au as well as the corresponding photoionization cross sections depend on the photon energy. For example, in the ultraviolet photoemission spectroscopy[24] (UPS) or x-ray photoemission spectroscopy[11,24] (XPS) ranges the Au elements are a few times greater than the corresponding Cu elements. On the other hand, the matrix-element effects do not influence the width of the PES

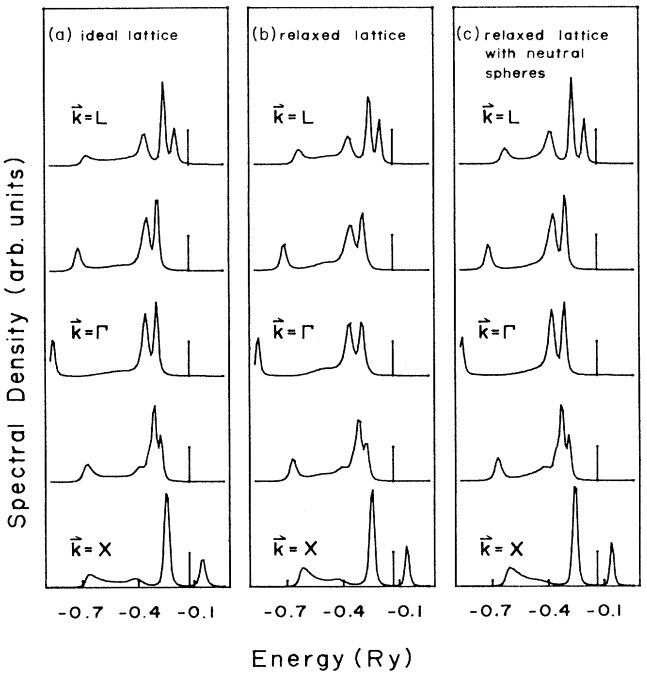

FIG. 5. Spectral densities of states for the disordered $Cu_{75}Au_{25}$ alloy evaluated for $\mathbf{k}$ points in the Brillouin zone of the face-centered-cubic lattice: $\mathbf{k}=(2\pi/a)(\frac{1}{2},\frac{1}{2},\frac{1}{2})\equiv L$, $\mathbf{k}=(2\pi/a)(\frac{1}{4},\frac{1}{4},\frac{1}{4})$, $\mathbf{k}=(2\pi/a)(0,0,0)\equiv\Gamma$, $\mathbf{k}=(2\pi/a)(\frac{1}{2},0,0)$, and $\mathbf{k}=(2\pi/a)(1,0,0)\equiv X$. The long vertical lines denote the position of the alloy Fermi level. Cases (a)–(c) are the same as in Fig. 2.

spectra (with the exception of too-low excitation energies). Another possible explanation for the band narrowing could be the surface effects as the escape depth of the photoelectrons depends on the excitation energy. This effect must, however, be similar for ordered and disorderd samples. One can also speculate on the possible effect of the short-range order in these alloys. Our model provides just the first simple scheme to tackle the problem and more experimental data concerning both the electron states and structure (e.g., EXAFS data) will be needed to refine it. Also, it is desirable to perform truly charge self-consistent CPA calculations within the models with different (neutral or almost neutral) sphere radii for the component atoms.

Regarding the spin-orbit coupling effects, the following conclusions can be drawn on comparison of semirelativistic and relativistic KKR-CPA calculations:[1,9,11] (i) The spin-orbit effects influence the lower part of the spectra dominated by Au d states and give rise to a dip there due to the splitting of Au $d^{3/2}$ and $d^{5/2}$ states (this is not present in our semirelativistic calculations); (ii) the width of the alloy spectra with and without the spin-orbit effects is essentially the same.

The spectral (Bloch) densities of states, which substitute the notion of the energy bands in disordered alloys,[16,17] are presented in Fig. 5 for all the studied models. It is instructive to compare this with the Cu and Au band structures for the potential parameters used in the alloy calculation (Fig. 6).

We see the upper parts of the Cu and Au bands intersect each other and thus in this energy region one should expect a virtual-crystal-like behavior. In other words, the corresponding peaks in the spectral density are only slightly broadened and describe an admixture of Cu and Au states.[2] On the other hand, the lower parts of the Cu and Au bands are significantly shifted with respect to each other, giving rise to two sets of levels in the alloy. Thus, in this energy region we observe strongly broadened well-separated peaks in the spectral density related to Cu and Au atoms. Note the different positions of Au-related d peaks for $\mathbf{k}=X$ or $\mathbf{k}=L$ around the energy

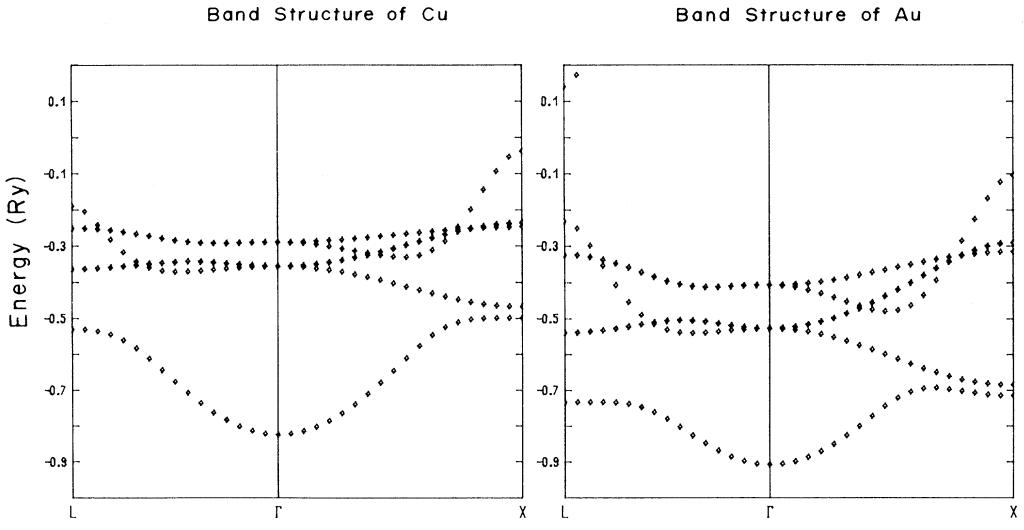

FIG. 6. Band structures of Cu and Au crystals along the line $L-\Gamma-X$ in the Brillouin zone of the face-centered-cubic lattice evaluated for the potential parameters used in the disordered alloy, case (c).

$E=-0.7$ Ry for models (a)–(c). This reflects the different Au d-band widths found in these models. The sharp peaks at $E\chi-0.85$ Ry for $\mathbf{k}=\Gamma$ or at $E\approx-0.12$ Ry for $\mathbf{k}=X$ correspond to the common virtual-crystal-like s band.

C. The $Cu_{75}Au_{25}$ alloy with LRO

Before discussing the results, it is worthwhile mentioning previous theoretical attempts to address the problem of LRO effects on the electronic structure of alloys. The electronic DOS in pseudobinary intermetallic compounds of the $(A_{1-x}B_x)_mC_n$ type was determined in Ref. 25 by combining the CPA and the recursion method based on a simplified TB model, in which only the site-diagonal disorder was taken into account. The KKR-CPA technique was recently applied to the problem of ordering on the simpler CsCl lattice for $Cu_{50}Zn_{50}$ (Ref. 26) and $Ag_{50}Zn_{50}$ (Ref. 27) alloys. In these calculations[26,27] the ordered phase was studied using the LMTO method and the resulting self-consistent ASA potentials were used as the muffin-tin potentials in the KKR-CPA calculation for the disordered phase. The transfer of potentials from space filling (hence overlapping) WS spheres in the LMTO-ASA calculation to the touching (nonoverlapping) muffin-tin spheres in the KKR-CPA calculation is inappropriate and can lead to a significant loss of accuracy when the component atoms differ appreciably in size. This drawback is remedied in our calculations, where both the ordered and the disordered phases are treated on equal footing via the LMTO-ASA method.

Figures 7 and 8 display the first *ab initio* study of the electronic structure of the partially ordered $Cu_{75}Au_{25}$ alloy. The potential parameters are LRO dependent, as discussed at the end of Sec. II. The $S=0$ limit corresponds to the model (c) in Figs. 2–4. The total DOS, Fig. 7, continuously interpolates between the ordered Cu_3Au alloy and its completely disordered phase. Nearly all features of the ordered-phase electronic structure are already washed out by disorder for $S=0.5$. The sublattice local Cu and Au DOS are plotted in Fig. 8. Note that Cu and Au sublattices become equivalent for $S=0$ because the concentrations of Cu and Au atoms on them are equal, unlike the case with $S=0$. The local Cu DOS on Cu and Au sublattices stay essentially the same except for a broadening as S decreases from 1 to 0. This is partly due to disorder and partly due to lattice relaxation, since for $S=0$ the Cu-Cu distances are close to that in the pure crystal and therefore smaller than the corresponding distances in the ordered Cu_3Au alloy. The local Au DOS on the Au sublattice broadens, as S changes from 1 to 0, due to disorder and the increasing possibility of the occurrence of nearest-neighbor Au-Au pairs with decreasing S (there are no nearest neighbor Au-Au pairs in ordered Cu_3Au). The local Au DOS on the Cu sublattice changes significantly, exhibiting a two-peak structure for $S>0.5$. Consider, for simplicity, just one "antisite" Au atom on the Cu sublattice in an otherwise perfect (-ordered) Cu_3Au alloy. While the Au atoms on the Au sublattice have twelve Cu atoms as their nearest neigh-

TABLE I. Potential parameters of Cu and Au atoms for the ordered Cu_3Au alloy obtained by the self-consistent LMTO method and constructed from tabulated (Ref. 20) pure-crystal values according to Ref. 19 (in parentheses).

	C (Ry)	Δ (Ry)	γ
		Cu	
s	−0.440	0.1602	0.4080
	(−0.443)	(0.1606)	(0.4085)
p	0.555	0.1422	0.1008
	(0.558)	(0.1436)	(0.1015)
d	−0.346	0.0073	−0.0024
	(−0.330)	(0.0075)	(−0.0028)
		Au	
s	−0.613	0.1363	0.4585
	(−0.615)	(0.1381)	(0.4580)
p	0.398	0.1775	0.1510
	(0.401)	(0.1771)	(0.1497)
d	−0.477	0.0240	0.0135
	(−0.483)	(0.0242)	(0.0140)

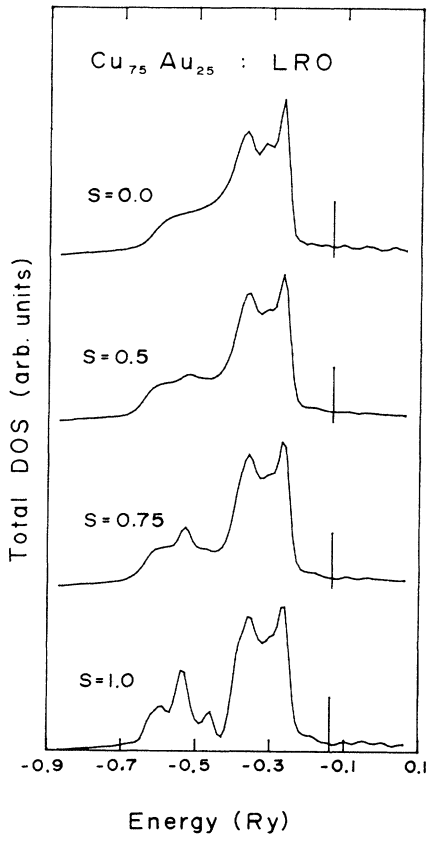

FIG. 7. Total density of states for the partially ordered $Cu_{75}Au_{25}$ alloy. The values of the long-range-order parameter S are ascribed to the corresponding curves. The long vertical lines denote the positions of the Fermi level.

bors, the Au atom on the Cu sublattice has four Au and eight Cu atoms as its nearest neighbors. This leads to a splitting in the local Au DOS. With increasing concentration of Au atoms on the Cu sublattice (i.e., with decreasing value of S) this effect becomes less pronounced and disappears entirely for the completely disordered case, when the local Au DOS on the Cu and Au sublattices become identical.

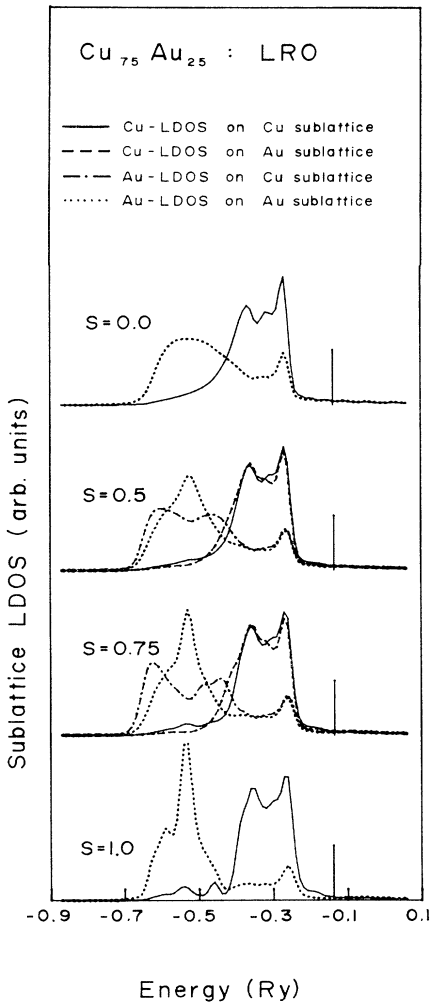

FIG. 8. Same as in Fig. 7, but for the sublattice local densities of states (LDOS): (i) the Cu LDOS on the Cu sublattice (solid lines), (ii) the Cu LDOS on the Au sublattice (dashed lines), (iii) the Au LDOS on the Cu sublattice (dash-dotted lines), (iv) the Au LDOS on the Au sublattice (dotted lines). In the completely disordered alloy ($S=0$) all sublattices are equivalent. The Cu and Au LDOS are then denoted by the solid and dotted lines, respectively. The values of the long-range-order parameter S are ascribed to the corresponding curves. The long vertical lines denote the positions of the alloy Fermi level.

D. Transferability of pure crystal parameters

The fact that the atomic spheres in the alloy, both ordered and disorderd, can be made neutral for radii close to the pure-crystal values, and that the sphere potentials are related to a common energy zero within the ASA are the basic reasons for the transferability of the LMTO potential parameters from pure Cu and Au to the Cu_3Au alloy. Of course, the pure-crystal parameters must be (unambiguously) modified, according to the prescription of Ref. 19, to take into account the slightly different sphere radii as well as the different WS radius for the alloy. Cu_3Au represents a difficult case from the standpoint of such a transferability of parameters in other schemes because of the significantly different sizes of the constituent atoms. It is generally believed that charge self-consistency is essential in such (e.g., Cu-Au, Cu-Pd) alloys. For example, the use of the pure-crystal Cu and Au phase shifts based on the Mattheiss construction in the KKR method required a rigid shift of the Au potential with respect to the Cu potential by 0.18 and 0.09 Ry in Refs. 2 and 11, respectively.

The results for the ordered Cu_3Au are summarized in Table I, where we compare the potential parameters [see Eq. (1)] obtained from the self-consistent LMTO method and by transferring parameters from pure Cu and Au according to the prescription of Ref. 19 (for sphere radii

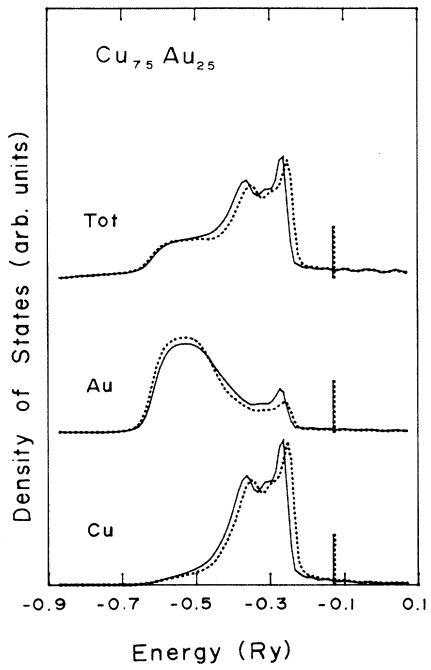

FIG. 9. Total and local Cu and Au DOS for the disordered $Cu_{75}Au_{25}$ alloy [model (b)] based on the potential parameters of the pure crystal constituents (Ref. 20) (solid lines) and on the potential parameters of the ordered Cu_3Au alloy obtained by the self-consistent LMTO method (dotted lines).

$s^{Cu}=2.670$ a.u. and $s^{Au}=3.012$ a.u.). The average energy deviations for one band at $\mathbf{k}=R,\Gamma,L$ points are less than 0.007 Ry, the maximum absolute value being 0.015 Ry. In Fig. 9 we compare the total and the LDOS for the completely disordered phase [case (c), $S=0$] based on the potential parameters obtained from self-consistent LMTO calculation for ordered Cu_3Au and from pure Cu and Au parameters appropriately modified for the alloy. The difference, which is small, is mainly due to the approximately 5% difference in the potential parameters C_d^{Cu} (see Table I), which determines the center of the Cu d band. Apart from that the agreement is excellent and justifies the transferability of the pure component parameters to the alloy calculation, especially in situations where the small loss in accuracy can be overlooked in view of the vastly reduced computing time and cost. It should be mentioned that even better agreement is obtained for Cu-Pd alloys.[15,28]

ACKNOWLEDGMENTS

J.K. and S.K.B. would like to acknowledge the warm hospitality of the members of Max-Planck-Institute, Stuttgart, where most of this work was carried out. S.K.B. would like to acknowledge partial financial support by the Natural Sciences and Engineering Research Council of Canada.

[1]R. G. Jordan, G. S. Sohal, B. L. Gyorffy, P. J. Durham, W. M. Temmerman, and P. Weinberger, J. Phys. F **15**, L135 (1985).
[2]H. Asonen, C. J. Barnes, M. Pessa, and R. S. Rao, Phys. Rev. B **31**, 3245 (1985).
[3]W. Eberhardt, S. C. Wu, R. Garrett, D. Sondericker, and F. Jona, Phys. Rev. B **31**, 8285 (1985).
[4]T. K. Sham, K. H. Tan, and Y. M. Yiu, Physica B **158**, 28 (1989).
[5]S. Krummacher, N. Sen, W. Gudat, R. Johnson, F. Grey, and J. Ghijsen, Z. Phys. B **75**, 235 (1989).
[6]T. K. Sham, Y. M. Yiu, M. Kuhn, and K. H. Tan, Phys. Rev. B **41**, 11 881 (1990).
[7]H. L. Skriver and H. P. Lengkeek, Phys. Rev. B **19**, 900 (1979).
[8]J. W. Davenport, R. E. Watson, and M. Weinert, Phys. Rev. B **37**, 9985 (1988).
[9]B. Ginatempo and J. Staunton, J. Phys. F **18**, 1827 (1988).
[10]P. Weinberger, A. M. Boring, R. C. Albers, and W. M. Temmerman, Phys. Rev. B **38**, 5357 (1988).
[11]B. Ginatempo, G. Y. Guo, W. M. Temmerman, J. B. Staunton, and P. J. Durham (unpublished).
[12]E. Arola, R. S. Rao, A. Salokatve, and A. Bansil, Phys. Rev. B **41**, 7361 (1990).
[13]N. Stefanou, R. Zeller, and P. H. Dederichs, Solid State Commun. **62**, 735 (1987).
[14]H. Wright, P. Weightman, P. T. Andrews, W. Folkerts, C. F. J. Flipse, G. A. Sawatzky, D. Norman, and H. Padmore, Phys. Rev. B **35**, 519 (1987).
[15]J. Kudrnovský and V. Drchal, Solid State Commun. **70**, 577 (1989).
[16]J. Kudrnovský, V. Drchal, and J. Mašek, Phys. Rev. B **35**, 2487 (1987).
[17]J. Kudrnovský and V. Drchal, Phys. Rev. B **41**, 7515 (1990).
[18]O. K. Andersen and O. Jepsen, Phys. Rev. Lett. **53**, 2571 (1984).
[19]O. K. Andersen, O. Jepsen, and M. Šob, in *Electronic Structure and Its Applications,* edited by M. Yussouff (Springer, Berlin, 1987), pp. 1–57.
[20]O. K. Andersen, O. Jepsen, and D. Glötzel, in Proceedings of the International School of Physics "Enrico Fermi," Course LXXXIX, Varenna, 1985, edited by F. Bassani, F. Fumi, and M. P. Tosi (North-Holland, Amsterdam, 1985), p. 59.
[21]T. Muto and Y. Tagaki, Solid State Phys. **1**, 193 (1955).
[22]S. Frota-Pessoa, Phys. Rev. B **28**, 3753 (1983).
[23]L. Goodwin, A. S. Skinner, and D. G. Pettifor, Europhys. Lett. **9**, 701 (1989).
[24]J. J. Yeh and I. Lindau, At. Data Nucl. Data Tables **32**, 1 (1985).
[25]J. Innoue and M. Shimizu, J. Phys. F **17**, 2067 (1987).
[26]W. M. Temmerman, P. J. Durham, Z. Szotek, M. Šob, and C. G. Larsson, J. Phys. F **18**, 2387 (1988).
[27]N. M. Harrison, P. J. Durham, and W. M. Temmerman, J. Phys. Condens. Matter **1**, 3315 (1989).
[28]S. K. Bose, J. Kudrnovský, O. Jepsen, and O. K. Andersen (unpublished).